Supporting Information for

Enhanced Catalytic and SERS Performance of Shape/Size Controlled Anisotropic Gold Nanostructures

Kamalesh Nehra,[1] Senthil Kumar Pandian,[1,*] Moram Sree Satya Bharati,[2] and Venugopal Rao Soma[2,#]

1 Department of Physics and Astrophysics, University of Delhi, Delhi11007, India

2 Advanced Centre for Research in High Energy Materials **(ACRHEM),** University of Hyderabad, Prof. C. R. Rao Road, Hyderabad 500046, Telangana, India

Corresponding Author e-mail: **soma_venu@uohyd.ac.in; soma_venu@yahoo.com**

* e-mail: senthupk@gmail.com

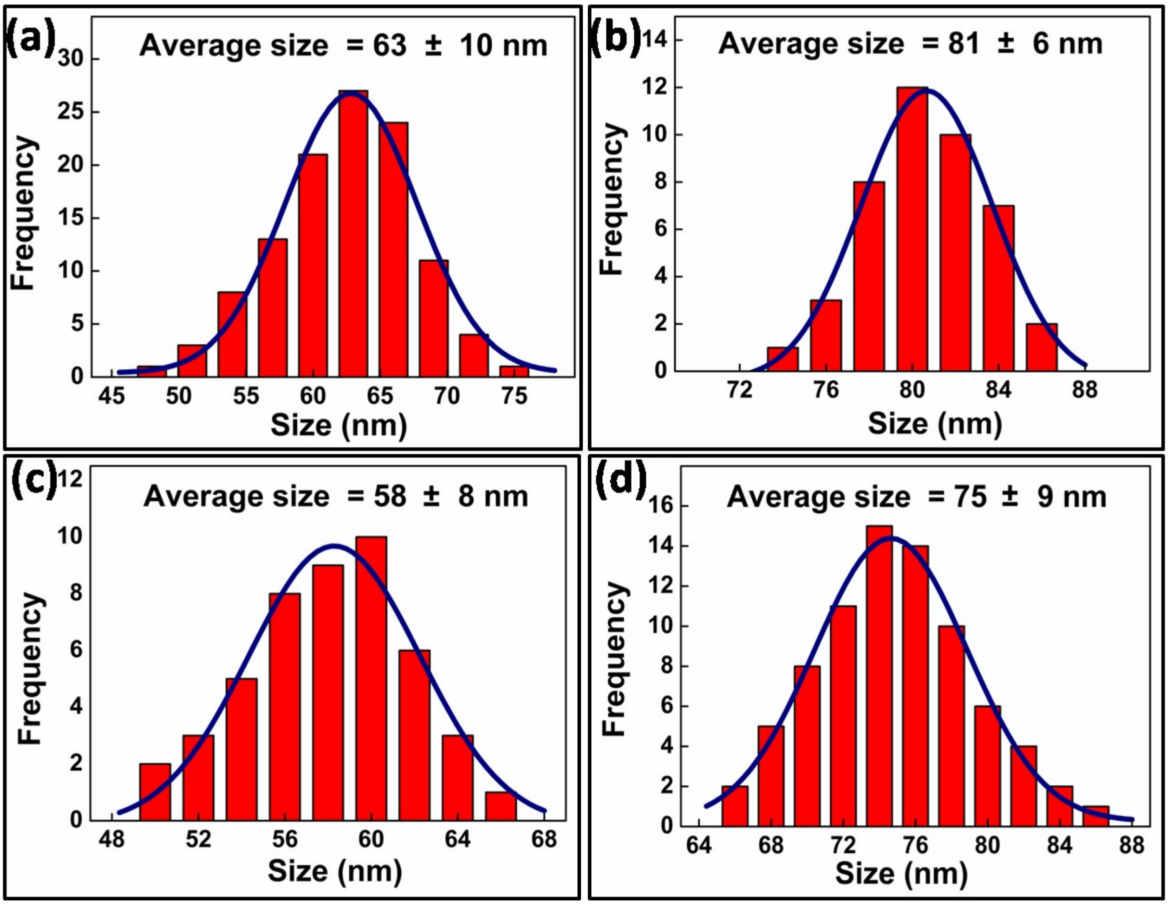

Fig. S1 Histogram of different shapes (a) spherical (b) decahedra (c) hexagonal and (d) star Au NPs respectively.

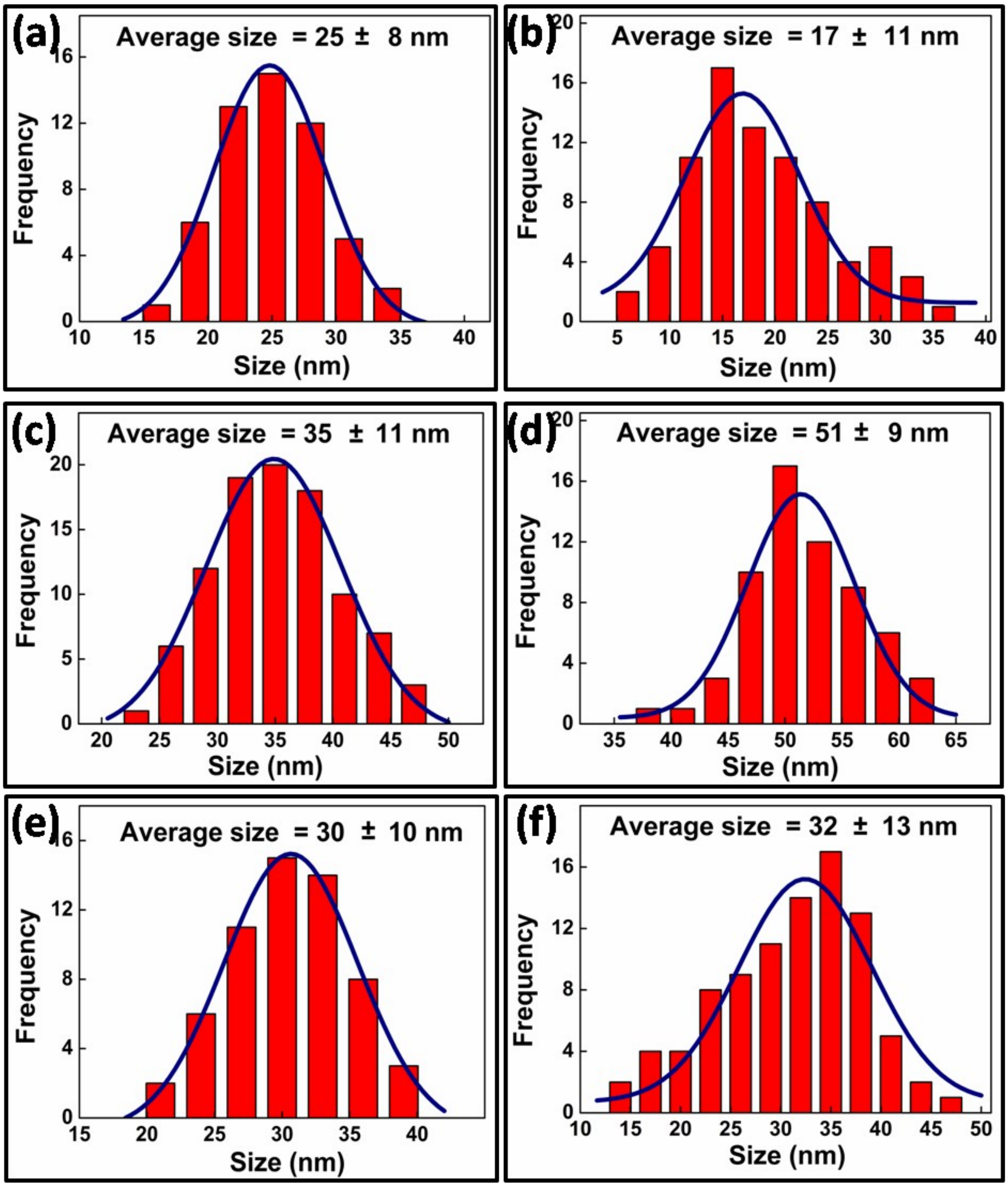

Fig. S2 Core size histogram of different star Au NPs (a) BK4, (b) BK7, (c) BK8, (d) BK9, (e) BK11 and (f) BK12 samples code respectively.

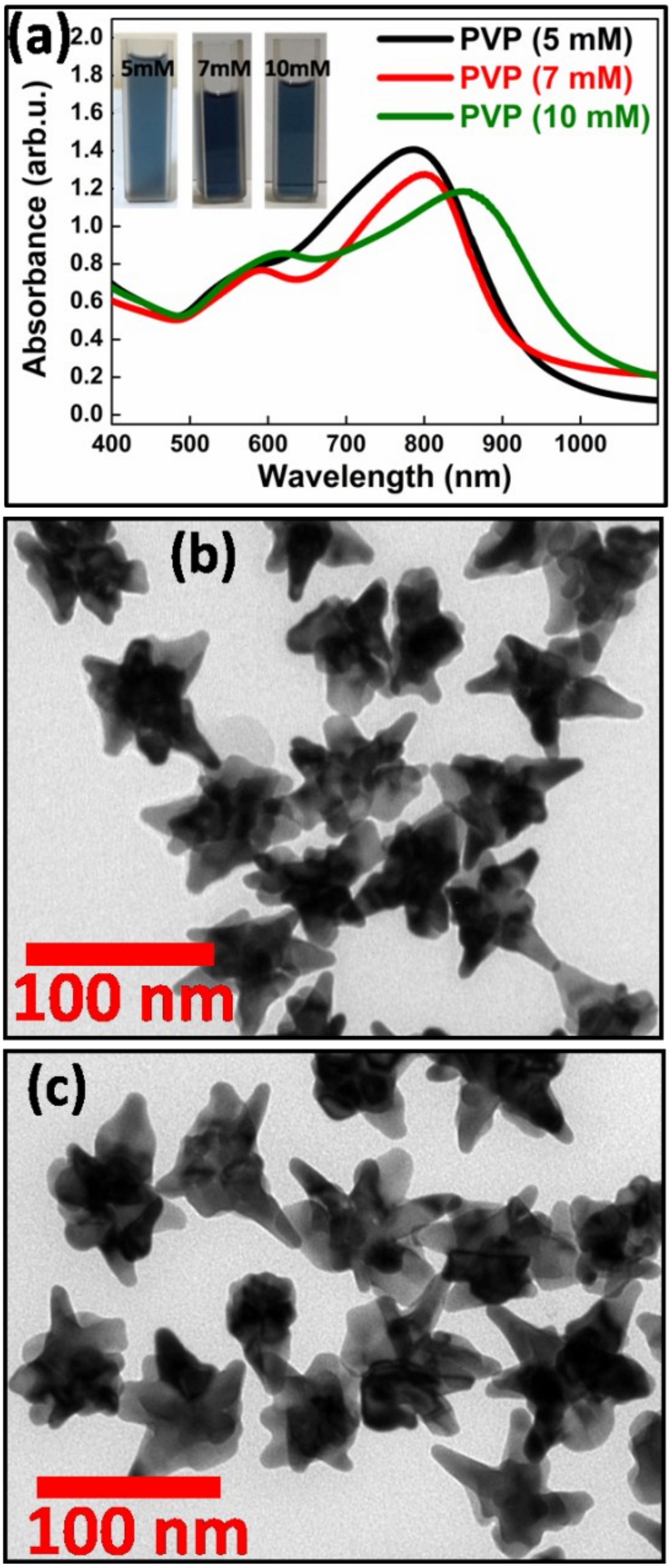

Fig. S3 UV-Vis absorption spectra Au NPs which synthesized with varying PVP concentration 5, 7 and 10 mM along with constant NaOH (1.5mM) and gold metal ions in DMF solvent. The color of these solutions showed in inset and Fig.(b) and (c) corresponding TEM images of 7mM and 10mM respectively.

Table S1: Peaks position of different facets in Au NPs with 2θ and their relative intensity.

Au NPs (Sample code)	<111> 2θ (^{0})	<200> 2θ (^{0})	<220> 2θ (^{0})	<311> 2θ (^{0})	<222> 2θ (^{0})	<200>/<111>	<220>/<111>	<311>/<111>	<222>/<111>
Methanol	38.36	44.58	64.94	77.81	81.73	0.33	0.19	0.16	0.06
Ethanol	38.35	44.48	64.58	77.44	81.74	0.27	0.12	0.08	0.06
2-Propanol	38.36	44.56	64.74	77.88	81.93	0.38	0.20	0.16	0.06
BK4	38.36	44.58	64.77	77.75	81.90	0.32	0.19	0.11	0.03
BK7	38.42	44.67	64.89	77.82	81.96	0.29	0.14	0.10	0.05
BK8	38.36	44.59	64.80	77.74	81.89	0.33	0.13	0.10	0.04
BK9	38.41	44.64	64.82	77.85	81.93	0.28	0.11	0.09	0.03
BK11	38.38	44.61	64.81	77.78	81.91	0.33	0.18	0.16	0.06
BK12	38.37	44.61	64.80	77.82	81.94	0.28	0.15	0.09	0.03

Crystallite size and Strain of all synthesized Au NPs:

XRD data (presented in Fig. 4 in manuscript) directly provides the peak positions as well as peak broadening of the respective Au NPs.

(i) Broadening due to crystallite size:

Broadening due to crystallite size is calculated by using Scherer Formula (based on the assumption of Gaussian peak profiles [1]

$$\beta = k\lambda/D\cos\theta \qquad \ldots(1)$$

where D is crystallite size(grain diameter), θ is diffraction angle, β is peak width at FWHM(in radians), λ is the wavelength of X-rays (1.54Å) and k = 1.0.

(ii) Broadening due to strain:

Broadening due to strain can be expressed as

$\beta_{strain} = \eta.\tan\theta$ ...(2)

where η is strain in material.

The total broadening due to size and strain is

$\beta = \beta(\textit{particle size}) + \beta(\textit{strain})$

$\beta = k\lambda/ D\cos\theta + \eta\tan\theta$ [from eq (1) and (2)]

$\beta\cos\theta = k\lambda/ D + \eta\sin\theta$ ...(3)

Eqn. (3) illustrates a linear relationship between $\beta\cos\theta$ and $\sin\theta$. Slope of the linear relationship provides the lattice strain (η) and intercept is equal to $K\lambda/D$.

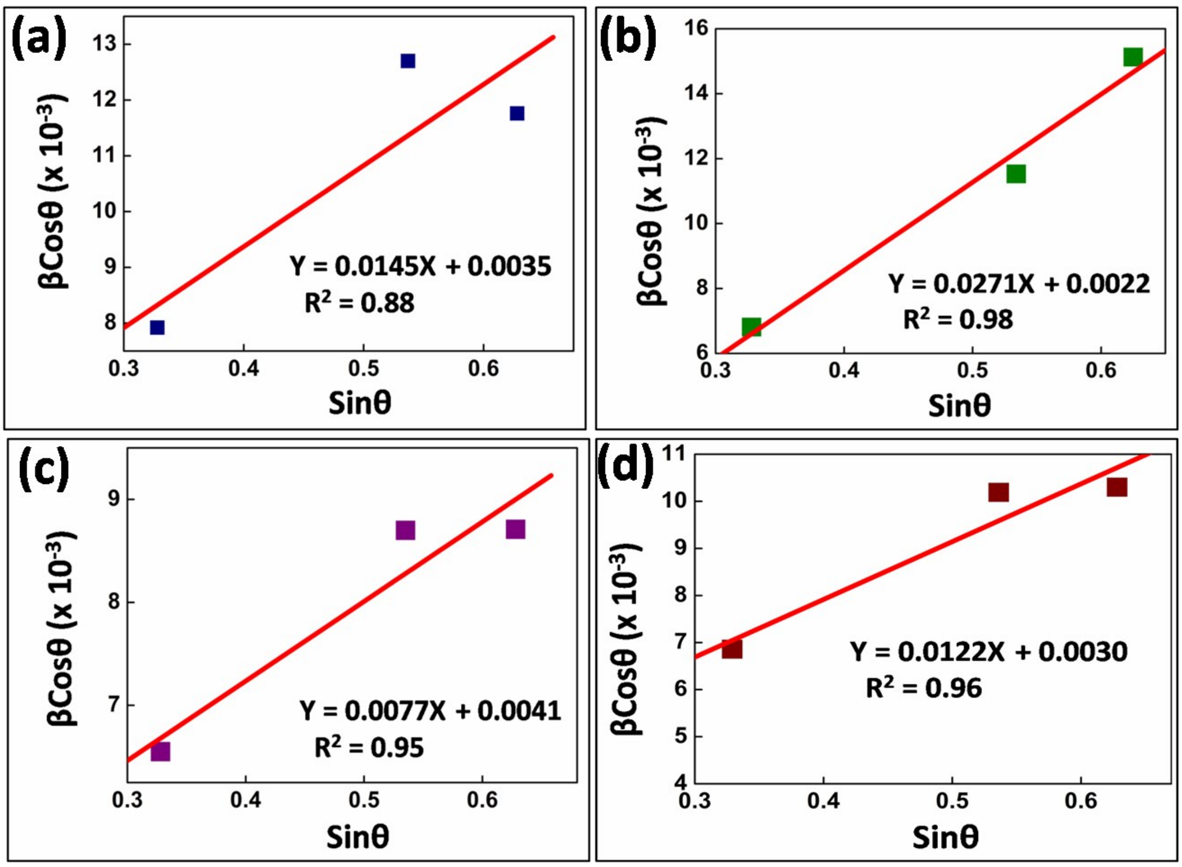

Fig. S4 Plots of $\beta\cos\theta$ vs. $\sin\theta$ for different shapes Au NPs (a) spherical, (b) decahedral, (c) hexagonal and (d) star Au NPs respectively.

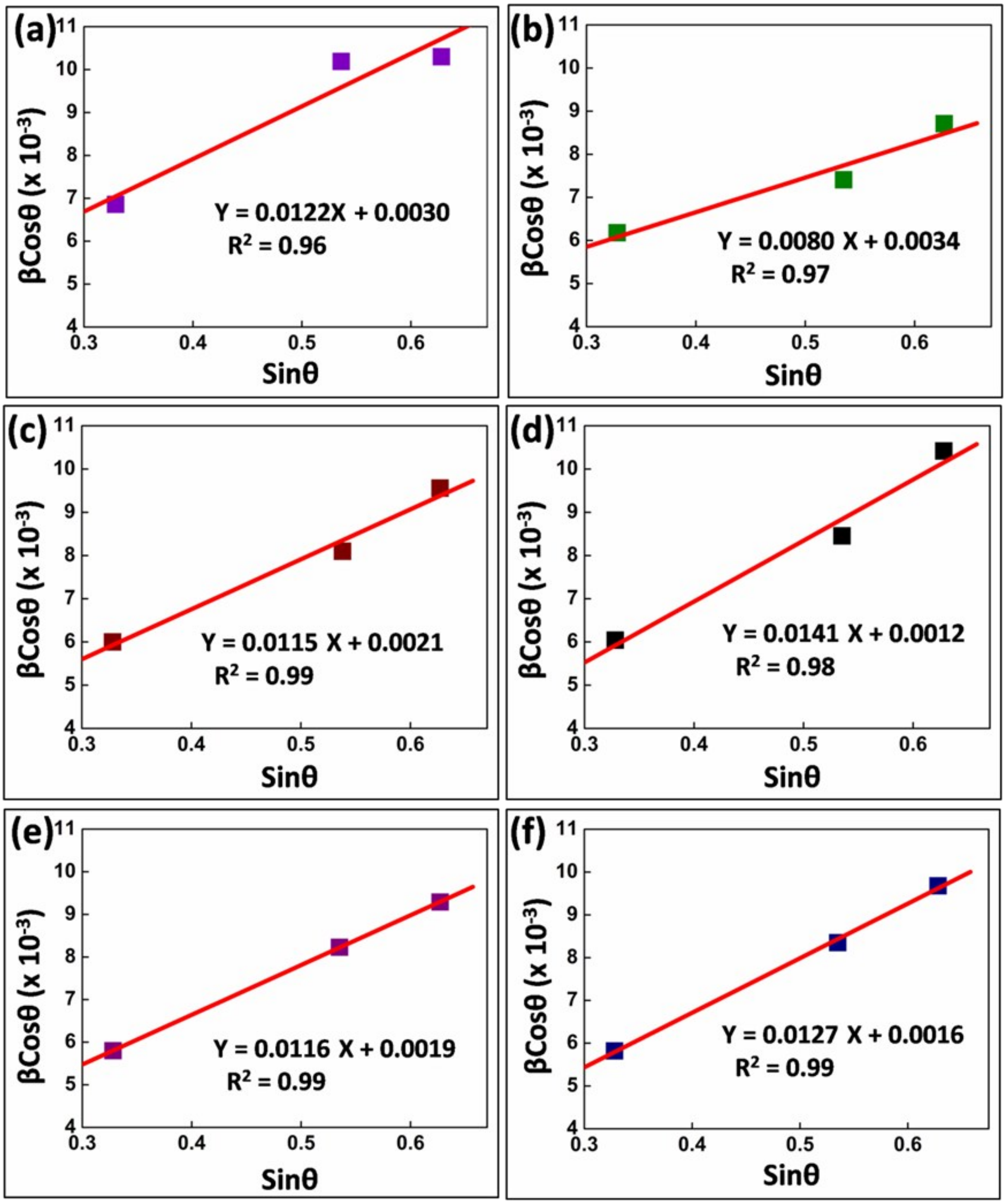

Fig. S5 Plots of βcosθ vs. sinθ for different star shape Au NPs (number of tips and tip to core ratio). (a), (b), (c), (d), (e) and (f) corresponding to samples code BK4, BK7, BK8, BK9, BK11 and BK12 respectively.

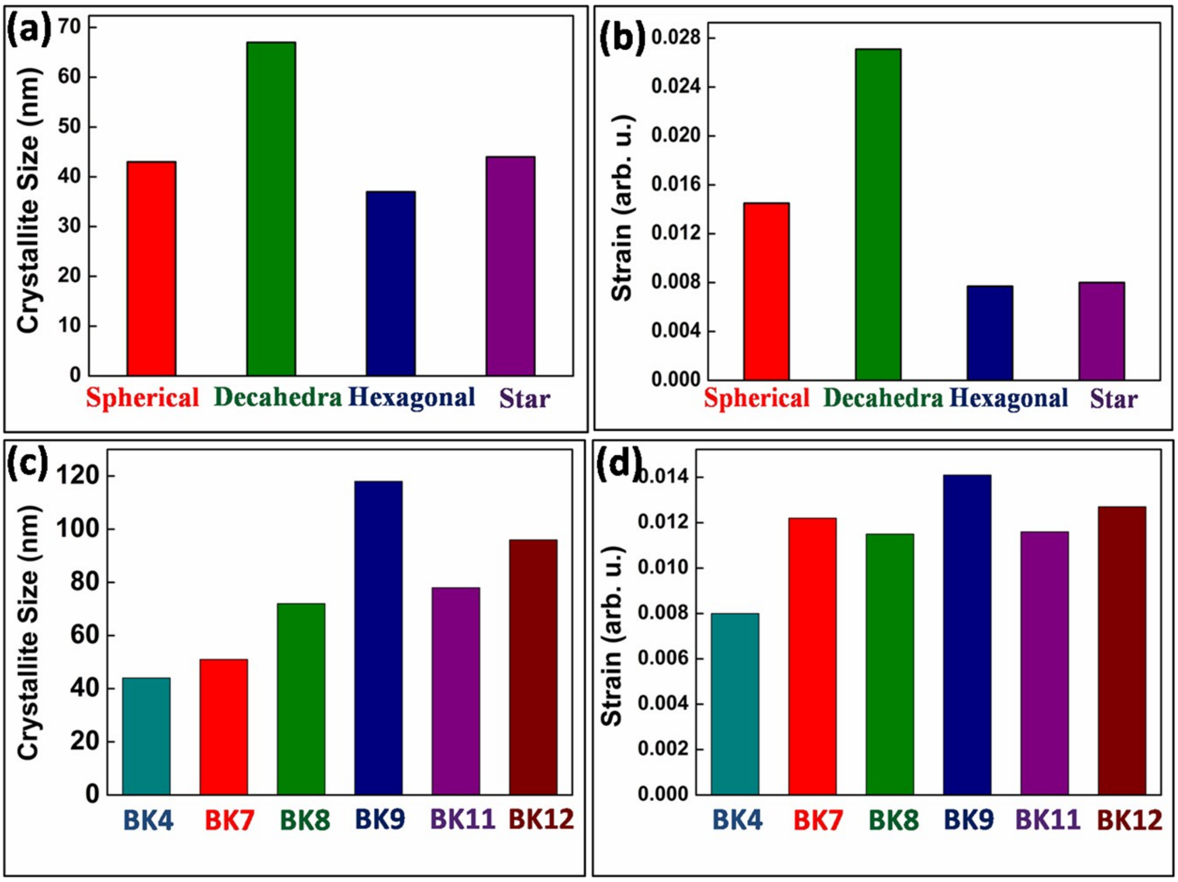

Fig. S6 Different shapes Au NPs (a) Crystallite size and (b) Strain. Different star shape Au NPs: (c) Crystallite size and (d) Strain.

As shown in figures S4 and S5, a graph is plotted between βcosθ and sinθ for different Au NPs to obtain the value of crystallite size and strain. Fig. S6 presents the crystallite size and strain calculated for these Au NPs. As observed in fig S6(a) and S6(b), crystallite size and strain were observed to be minimum in hexagonal Au NPs in comparison with other shapes. In star shaped Au NPs, crystallite size was slightly more and strain was comparatively less. Figures S6(c) and S6(d) show the size and strain in different number of tips and tip to core ratio star Au NPs. We observed that in BK4 and BK8 samples, strain was less compared to other samples.

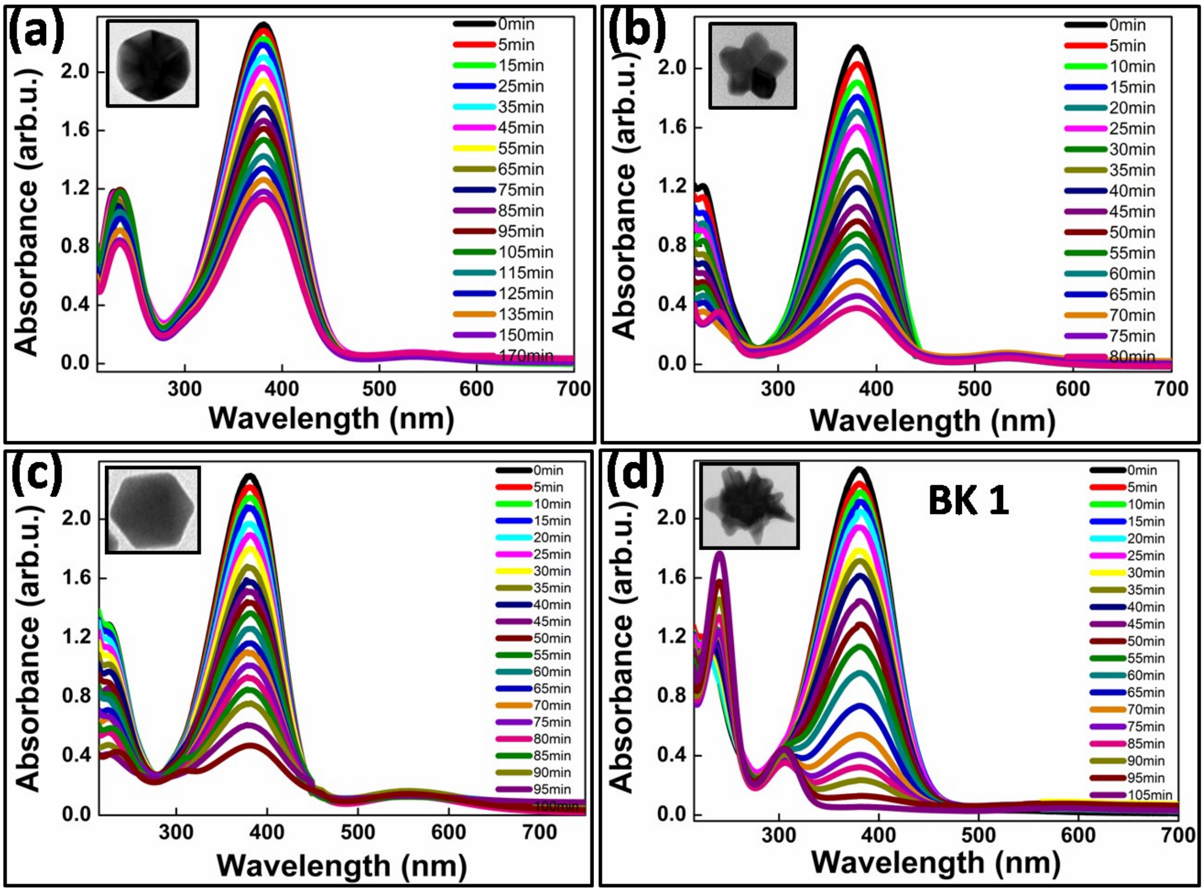

Fig. S7 Reduction kinetics of p-NA in the presence of different shapes Au NPs (a) spherical, (b) decahedron, (c) hexagonal and (d) star shape (BK 1 is the sample code) respectively.

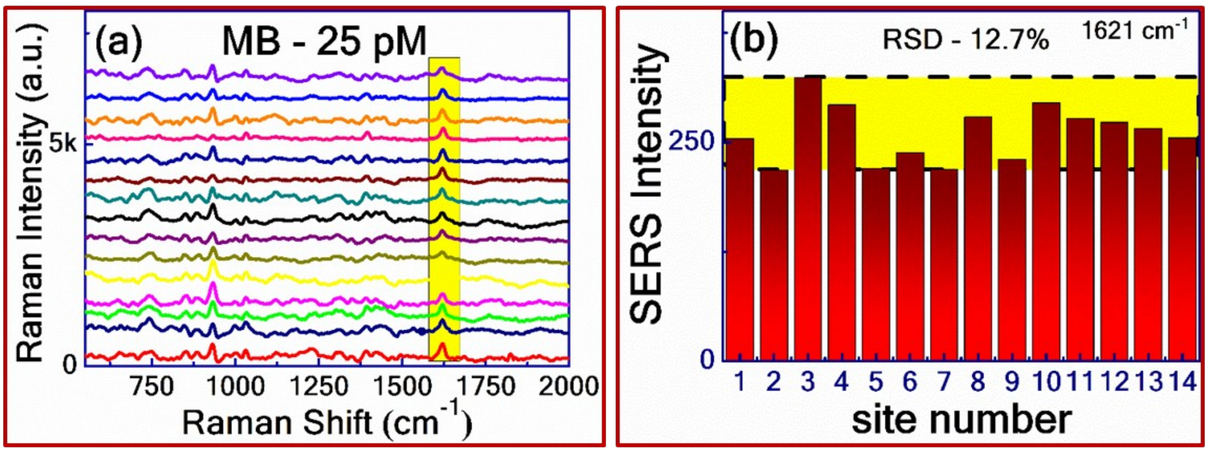

Fig. S8 (a) SERS spectra of MB using BK8 NPs recorded multiple times at different sites and (b) SERS intensity of 1624 cm^{-1} peak.

References:

1. H. P. K. Leroy Alexander, *Journal of Applied Physics*, 1950, **21**.